

Error Elimination Algorithm in 3D Image Reconstruction

Jin Xian-Hua^{1*}, Zhao Yuan-Qing²

¹Computer Teaching Department, Anyang Normal University, Anyang Henan 455000, China

²School of Computer and Information Engineering, Anyang Normal University, Anyang 455000 china;

*Corresponding author, e-mail: yuanqing_zhao01@163.com¹

Abstract

In process of three-dimensional (3D) reconstruction, effective matching of feature is the key point of accurate reconstruction in later stage. In order to eliminate the error of modeling distortion caused by inaccurate feature matching in the process of 3D image reconstruction, a feature matching error elimination method based on collision detection is presented. A 3D image reconstruction mathematical model is established to operate the solution of image 3D reconstruction and camera space matrix elements of exterior orientation. The error of the feature matching in 3D dynamic modeling is eliminated according to the result of the collision two gray digital images are used to carry out simulation experiment. Experimental results show that the proposed algorithm can effectively eliminate the error of feature matching and improve the accuracy of the modeling.

Keywords: 3D reconstruction, elements of exterior orientation, camera calibration, gray level image

Copyright © 2014 Institute of Advanced Engineering and Science. All rights reserved.

1. Introduction

The objective world is three-dimensional space, but the images acquired by existing technology is two-dimension, three-dimension reconstruction technique is proposed to obtain 3D information and make reasonable expression of 3D information possible. 3D reconstruction is the most important field of computer vision research [1, 2]. The goal is to make the computer has the ability of cognizing 3D environmental information through the 2D image, including the perception of geometric information of objects in the 3D environment, such as the shape, position, posture, etc., and can describe, store, recognize and understand them. With the continuous development of computer science and technology, image-based 3D reconstruction has been widely used in industrial measurement, architectural design, entertainment, archaeological, e-commerce, medical image processing and other fields.

For issues related image matching in 3D reconstruction process, researchers have proposed a number of solutions [3]. Literature proposed a hierarchical image matching modeling algorithm based on wavelet transformation, interest points extracted from each layer of the image decomposition are matched, with parallel strategies to improve the computing speed, however, the special priori requirement is set up as premise to the assuming that algorithm can effectively extract interest points, and limit its application. Feature-based method extract feature space from the images waiting to be matched firstly, match the images based on the use of the correspondence between features [4, 5]. The method utilizes the salient features of the image, with a small amount of calculation, fast speed and other characteristics, has a certain robustness of the image distortion, noise and occlusion, but the matching performance depends largely on feature extraction quality. If the pixel quality is low, it will result in the matching error occurs, so as to lead to error in post-modeling [6, 7].

To solve this problem, this paper introduces the feature matching error elimination algorithm based on pixel error collision detection, in the case of solving linear and nonlinear, the error component, calibration interval composed of pixel error, detect collision behavior of mathematical models caused the error in the process of pixel correspondence, and operate simulation experiment of reconstruction, in order to eliminate feature matching error during the process of 3D reconstruction, and improve the precision and accuracy of modeling [8, 9].

2. Image Feature Matching in 3D Image Reconstruction Process

Image feature matching calculates the corresponding relationship of feature points extracted from the left and right images by a certain standard. First, select the appropriate primitive, and then get the correspondence relationship between the primitives of two images by calculating. As shown in Figure 1, x is the point that space point X of 3D image projected onto the primary image, and C is the optical center of the camera. P represents the projection matrix of this image, $P^+ = P^T (PP^T)^{-1}$ is the inverse matrix of P . Because that point P^+x satisfy the equation $x = PX$, P^+x and C are both on the projection line of spatial point X .

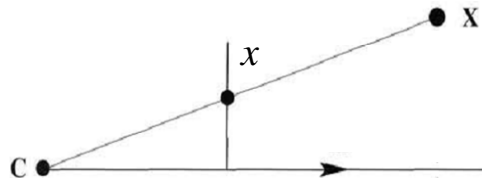


Figure 1. The Epipolar Geometry Relationship of Single Image

As shown in Figure 2, the projection point of C on the second image is e' . Assuming that P' is the projection matrix of the 2nd image, we can obtain the follow equation:

$$e' = P'C \tag{1}$$

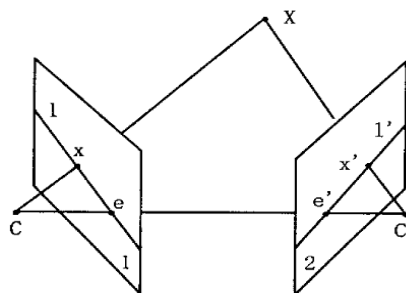


Figure 2. The Epipolar Geometry Relationship of Two Images

Point P^+x is on the epipolar geometry line l' of 2nd image, according to projection principle we can obtain:

$$l' = (P'C) \times (P'P^+x) = [e']_{\times} (P'P^+)x \tag{2}$$

Then we get the follow equation:

$$F = [e']_{\times} (P'P^+) \tag{3}$$

According to the assumption that the origin of the world coordinate is the center of the 1st image, then the projection matrixes of the two images are:

$$P = K [I | 0] \quad P' = K' [R | t]$$

Then, we can obtain that:

$$C = \begin{pmatrix} 0 \\ 1 \end{pmatrix} \quad P^+ = \begin{bmatrix} K^{-1} \\ 0^T \end{bmatrix} \quad (4)$$

Take Equation (4) into (3), the result is shown as follow:

$$F = \begin{bmatrix} e' \\ \times \end{bmatrix} P^+ P^+ = \begin{bmatrix} P^+ C \\ \times \end{bmatrix} P^+ P^+ = \begin{bmatrix} K^T t \\ \times \end{bmatrix} K^T R K^{-1} = K^{-T} \begin{bmatrix} t \\ \times \end{bmatrix} R K^{-1} \quad (5)$$

E is the key matrix, $E = \begin{bmatrix} t \\ \times \end{bmatrix} R$. The relationship of E and fundamental matrix F is described as Equation (6):

$$E = K^T F K \quad (6)$$

The 3D conversion is performed according to the corresponding relationship to complete the image reconstruction. From the reconstruction principle mentioned above, it can be seen that traditional reconstruction method completes the coordinate matrix transformation and the reconstruction based on the geometric characteristics or pixel gray feature. However, it is difficult to ensure the accuracy of the feature matching in the process of 3D image reconstruction, and a larger error occurred in the process of matching will cause the deviation of the image projection matrix, resulting in false matching when calculating the feature correspondence relationship, larger error for reconstruction, distortion and so on [10, 11].

3. Error Elimination Algorithm for Conflict in Feature Matching

3.1. Collision Detection

When the camera parameters are obtained, combined with the acquired feature points, a mathematical virtual model can be established. The virtual model is then used to represent the error of feature matching and adjusted, so as to complete the error elimination of the matching and lay a good foundation for the latter part of the modeling. The calculation process of the error elimination algorithm is as follows [12-14].

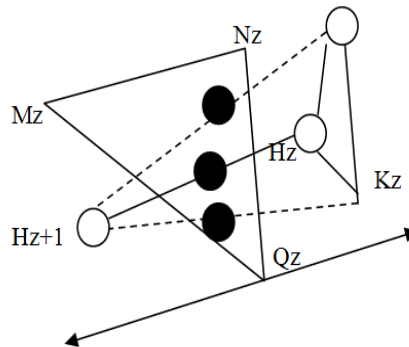


Figure 3. Schematic for Feature Point Collision Error Matching Detection

A virtual mathematical calibration area, which is an irregular polygon area, is formed based on many processes of pixel matching. Taking one random match point as the vertex, and when the coordinate value of the vertex is achieved, the associated corresponding relationship between the vertex and other pixel matching points should be constructed, so as to obtain the 2D coordinate area of the pixel points which may cause a match conflict error area, and build stable feature points matching relationship between vertices through vertex collision. The coordinates of the vertices are matched based on selection to build the mapping relationship between the corresponding vertex and the characteristics of the gradual changing area. Through the mapping relationship, the corresponding coordinates of the feature points which

may cause matching error can be determined clearly, and the measure standard is whether there is a collision phenomenon among the image pixels feature points of the error area. If so, errors will be produced. The schematic for collision detection of feature points is shown in Figure 3.

$\Delta M_z N_z Q_z$ and $\Delta H_{z+1} K_z G_z$ in Figure 3 denote the sensitive gradient range where the matching error phenomenon may occur, and the range describes the correlation of the corresponding self-cross detection coordinates. If the point H_z represents the diagonal cross point, and, at the same time, through the midpoint of $\Delta M_z N_z Q_z$, it is possible to obtain the spatial position correlation of the two gradient triangle ranges in accordance with the relationship between $\underline{X}_F \bullet \underline{n}$ and $\underline{X}_H \bullet \underline{m}$, as is shown in formula (7).

$$\begin{cases} \underline{X}_G = \underline{G}_z - \underline{M}_z \\ \underline{X}_H = \underline{H}_{z+1} - \underline{M}_z \\ \underline{X}_G^m = (\underline{X}_z \bullet \underline{m}) \underline{m} \\ \underline{X}_H^m = (\underline{X}_H \bullet \underline{m}) \underline{m} \end{cases} \quad (7)$$

Here, \underline{X}_G^m denotes the direction vector of \underline{X}_G , while \underline{X}_H^m indicates the direction vector of \underline{X}_H . Through the analysis of the correlation of $\underline{X}_G \bullet \underline{m}$ and $\underline{X}_H \bullet \underline{m}$, if the signs of the two characteristic data values are different, then the line formed by point H_z and point H_{z+1} is intersecting or tangent with $\Delta M_z N_z Q_z$. Some collisions will arise in the connections of the feature points in the gradient range, that is, errors exist in the match of the two. Therefore, 2D coordinate (x, y) of the matching point can be obtained based on the corresponding collision phenomenon, and then be adjusted to eliminate the error and ensure the accuracy of matching.

3.2. Calculation for the Exterior Orientation Elements

The matching error are achieved, from equation $E = [t]_x R$ we obtain that the key matrix, relating to the exterior orientation elements of the camera, can be decomposed to calculate rotation matrix R and translation matrix.

Large amount of experimental studies show that one of the key matrix eigenvalue is zero and the other two are equal. Therefore, $E = U \text{diag}(1 \ 1 \ 0) V^T$ can be got after decomposing the key matrix.

Solve the equation $E^T t = 0$, $t = \pm U \begin{pmatrix} 0 & 0 & 1 \end{pmatrix}^T = \pm u_3$ can be obtained.

$$W = \begin{bmatrix} 0 & -1 & 0 \\ 1 & 0 & 0 \\ 0 & 0 & 1 \end{bmatrix}$$

Assuming rotation matrix is W , through equation $R^T E^T = t^T$, we know that rotation matrix is represented as $R = UWV^T$ or $R = UW^T V^T$.

Key matrix E is known, based on the assumption that the projection matrix of the 1st image is $P = K [I | 0]$, there are following four possible projection matrixes for the 2nd image:

$$\begin{aligned} P' &= [UWV^T \quad | \quad +u_3] \\ &= [UWV^T \quad | \quad -u_3] \end{aligned}$$

$$\begin{aligned}
 &= \begin{bmatrix} UW^T V^T & | & -u_3 \end{bmatrix} \\
 &= \begin{bmatrix} UW^T V^T & | & -u_3 \end{bmatrix}
 \end{aligned}
 \tag{7}$$

Figure 4 shows the four possible projection matrixes. The difference between (a) and (b) is that the translation vector of the 1st camera is inverted to the one of the 2nd camera. The difference between (a)&(c) and (b)&(d) is inverted baseline. The difference between (a)&(b) and (c)&(d) is that camera B rotated 90° around the baseline. Therefore, only in (a) are the reconstruction point in front of the two cameras. That is to say, the exact projection matrix can be found from the four results by verifying whether a spatial point is in front of both the two cameras.

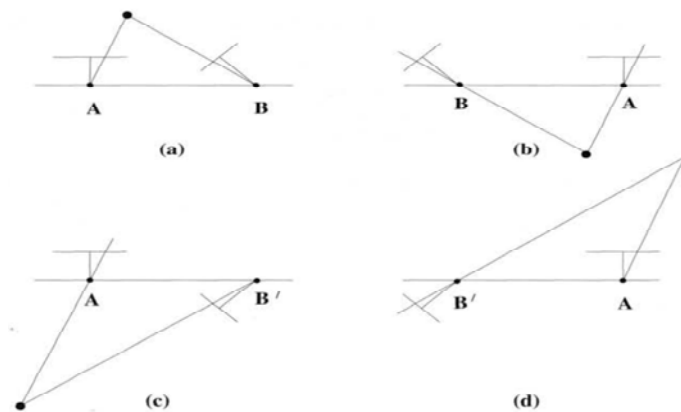


Figure 4. The Four Possible Projection Matrixes

3.3. The Solution for 3D Coordinate of the Points

The algorithm to solve the 3D coordinates can mainly be divided into two types: linear and nonlinear. Lots of parameters related to nonlinear method could increase the amount of computation and complexity and lead to cumulative error occurred to results. So this article adopts linear method to calculate the coordinate of 3D spatial points, and then uses least-squares constraint method for correction. The method is simple, but may get error result: local optimal result.

4. Experimental

4.1. Camera Calibration Experiment

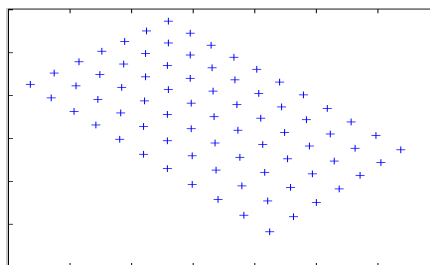


Figure 5. Feature Points Based on Harris Corner Detection Method

The calibration of Tsai camera is fulfilled in the MATLAB platform in this paper. In this experiment, the Cannon A75 digital camera is used to obtain the face image, and the size of the acquired image is 2048×1536 pixels, the size of the pixel unit is 0.002578×0.002578mm. The

calibration template is a printed 8×12 checkerboard-like paper, and the size of each grid is 20×20 mm. Figure 5 are the captured calibration template image and the feature points extracted by using Harris corner detector respectively.

The calibration results are as follows:

Effective focal length $f = 9.4223\text{mm}$

Distortion factor $k = 0.0020$

Transformation matrix R and T are:

$$\mathbf{R} = \begin{bmatrix} -0.6925 & 0.7131 & 0.1094 \\ 0.5282 & 0.6044 & 0.5964 \\ -0.4914 & -0.3552 & 0.7952 \end{bmatrix}, \quad \mathbf{T} = \begin{bmatrix} -21.1152 \\ -104.9076 \\ 767.5377 \end{bmatrix}$$

Using the calculated camera as model in the experiment, the interior orientation elements are:

$$\mathbf{K} = \begin{bmatrix} 1075.44385 & 0 & 497.71314 \\ 0 & 1078.01663 & 396.83714 \\ 0 & 0 & 1 \end{bmatrix}$$

4.2. Simulation Experiment for Reconstruction

Based on the proposed algorithm, the reconstruction experiment is carried out. First, the experiment is performed for two images, and the results are shown in Figure 6.

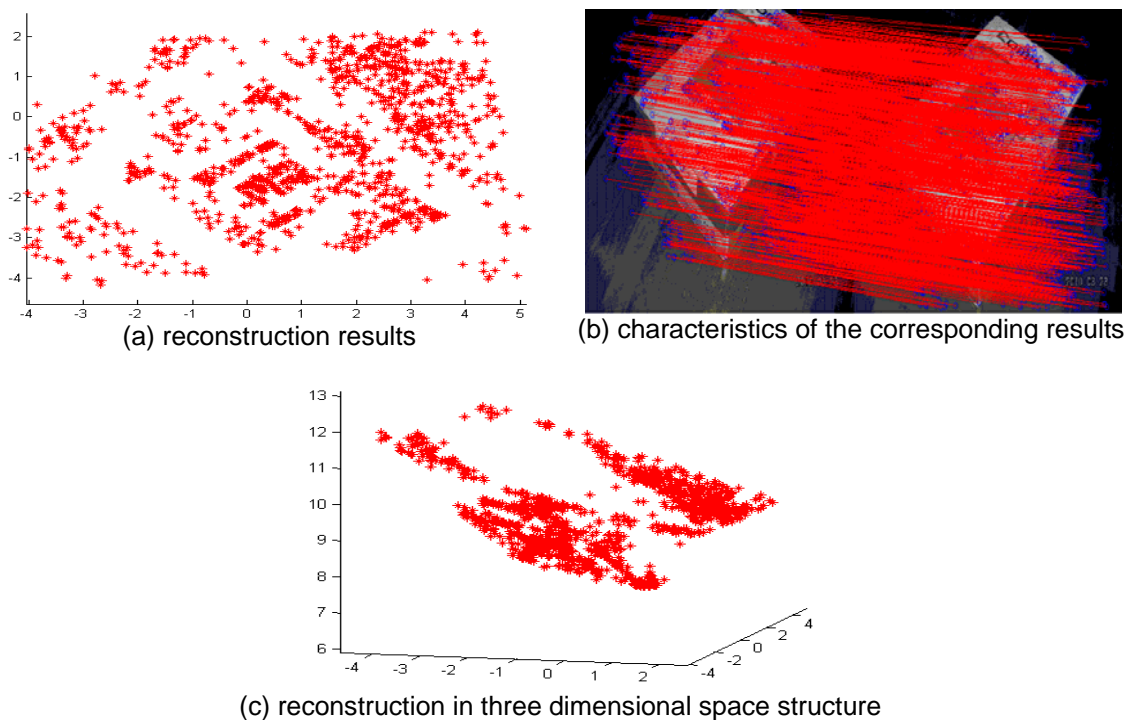


Figure 6. 3D Reconstruction Based on Two Images

Table 1. The Error of Reverse Projection

Anti-error	1st image	2nd image	3rd image	4th image	5th image
Max error x	0.5736	0.5453	0.5649	0.2952	0.2239
Min error y	0.3071	0.3136	0.9759	0.9548	1.0390
Ave error x	0.1289	0.1221	0.1562	0.0599	0.0630
Ave error y	0.0631	0.0641	0.2700	0.2596	0.2950

Table 2. Experimental Time

Dense matching	Reconstruction	Optimization	Time consumed	Number of points
33×4 min	2+3×4 min	4×4 min	162min	44349

Table 1 and 2 show the experimental results. Due to the relatively large perspective transformation between the first image and the second image, the number of matching points is fewer, the accuracy of the fundamental matrix is lower, thus, lead to the back-projection error getting larger. As a result of the optimization using error elimination method, there is no significant growth of the back-projection error in the fourth image and the fifth image. Accordingly, in the case of higher precision of camera calibration, the algorithm will not affect the subsequent image reconstruction when there is a larger error in the intermediate image.

5. Conclusion

The paper introduced the collision detection algorithm. It is demonstrated that the error of mismatch in image feature matching is better eliminated and the three-dimensional reconstruction of the entire model is achieved. It basically meets the dimensional image reconstruction for its stable and reliable, high precision, anti-interference ability. Furthermore, it provides a theoretical reference for errors elimination of feature matching in three-dimensional image reconstruction and provides strong support for the in-depth study of three-dimensional image reconstruction. It also has a certain practicality in application field.

References

- [1] VA Syrovoy. Formation of arbitrary axisymmetric relativistic beams. *Journal of Communications Technology and Electronics*. 2013; 58(2): 165-171.
- [2] VV Solov'ev. Implementation of finite-state machines based on programmable logic ICs with the help of the merged model of Mealy and Moore machines. *Journal of Communications Technology and Electronics*. 2013; 58 (2): 172-177.
- [3] AV Klyuev. Detection of a random process with the use of a doped Schottky diode. *Journal of Communications Technology and Electronics*. 2013; 58(2): 178-184.
- [4] AS Petrov, VV Makeev. Analysis of the characteristics of microstrip antennas in the decimeter wave range. *Journal of Communications Technology and Electronics*. 2013; 58(3): 185-195.
- [5] ZHANG Yan, REN An-hu. Research on Multiple Feature and BP Neural Network Licence Plate Recognition System. *Science Technology and Engineering*. 2012; 12(22): 5645-5648.
- [6] TI Bichutskaya, GI Makarov. Cylindrical irregularity on a half-space and equivalent radiators. *Journal of Communications Technology and Electronics*. 2013; 58(3): 196-202.
- [7] AM Bobreshov, II Meshcheryakov, GK Uskov. Optimization of the geometry of a TEM-horn for radiation of ultrashort pulses used as an element of an antenna array with controlled position of the main lobe. *Journal of Communications Technology and Electronics*. 2013; 58(3): 203-207.
- [8] SHEN Xiao-lei, ZHOU Wu-neng. Compressed Sensing and Its Application in License Plate Recognition System. *Science Technology and Engineering*. 2012; 12(19): 4797-4803.
- [9] KS Kalashnikov, BI Shakhtarin. Estimation and compensation for the influence of interchannel interference in reception of OFDM signals. *Journal of Communications Technology and Electronics*. 2013; 58(3): 208-216.
- [10] SG Kalenkov, GR Lokshin. Modulation microscopy and nonmonochromatic light hologram recording. *Journal of Communications Technology and Electronics*. 2013; 58(3): 217-220.
- [11] SV Savel'ev. Bifurcation effects with additively increasing period of oscillations in a system with one and a half degrees of freedom. *Journal of Communications Technology and Electronics*. 2013; 58(3): 221-225.
- [12] YAO Zhi-ying. Research on Highway-Tunnel Traffic Alarming Based on License Plate Recognition. *Logistics Technology*. 2009; 28(4): 78-79.
- [13] VM Kotov, GN Shkerdin, VI Grigor'evskii. Polarization features of the 2D contouring of an optical image under double Bragg diffraction conditions. *Journal of Communications Technology and Electronics*. 2013; 58(3): 226-232.
- [14] Zi-Yu Ma, Da-Wei Li, Fang-Wu Dong. Gross Error Elimination Based on the Polynomial Least Square Method in Integrated Monitoring System of Subway. *International Journal of Electrical and Computer Engineering*. 2013; 12(1): 366-371.